5

Infrared Thermography – Applications in Poultry Biological Research

S. Yahav and M. Giloh
Institute of Animal Science,
ARO the Volcani Center, Bet-Dagan
Israel

1. Introduction

Infrared (IR) thermal imaging technology has undergone major development during the past decade. Since 2000 this technology has been developed rapidly, through use of automated systems which have become widely available and cheaper as the technology developed (FLIR Systems, 2004).

Infrared thermal imaging cameras (IRTIC) measure the amount of near-IR radiation – characterized by wavelength of 8 to 12 μm – that is emitted from a surface, and convert it to a radiative temperature reading, according to the Stefan-Boltzmann equation:

$$R = \varepsilon\sigma T^4$$

where ε is the emissivity of the surface, which is defined as the ability of a surface to emit and absorb radiation, and which, for biological surface tissues, ranges between 0.94 and 1.0 (Hammel, 1956; Monteith & Unsworth, 1990); σ is the Stefan-Boltzmann constant (5.67×10^{-8} $Wm^{-2}K^{-4}$); and T is the surface absolute temperature in kelvins (K).

The images that visualize the temperature can be displayed in gray or colors (Figure 1), and can be analyzed as spots (1 spot = 1 pixel) or as user-defined Regions of Interest (ROI), by means of a special computer program.

The IRTI technique plays a major role in biological research applications such as: thermal physiology in mammals (Klir & Heath, 1992; Klir et al., 1990; Mohler & Heath, 1988; Philips & Heath, 1992) and birds (Philips & Sanborn, 1994; Stewart et al., 2005; Yahav 2009; Yahav et al., 1998, 2004); fever diagnosis in homeotherm birds and mammals, including humans (Chiu et al., 2005; Nguyen et al., 2010; Teunissen & Daanen, 2011); cancer diagnosis (Cetingul & Herman, 2010; Herman & Cetingul, 2011; Kontos et al., 2011); and animal population counts.

The major advantage of IR is that it is a non-invasive and contact-free method of measuring surface temperature, at either short or relatively long distance, depending on the goal of the thermal study. For any thermal study: a thermal resolution of 0.1°C is recommended; and spatial resolution must be sufficient and appropriate for the size of the studied object and its distance from the IRTI camera. In general, a spatial resolution of 320 × 240 pixels – as

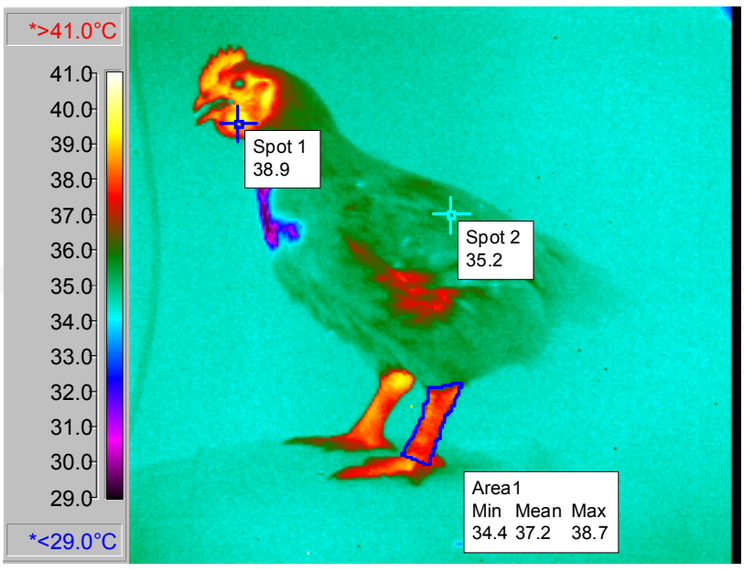

Fig. 1. Thermal image of a broiler chicken exposed to 35°C. The blue outline on the leg defines an ROI that comprises a section of surface area for which minimum, average and maximum surface temperatures were determined. Spots 1 and 2 exhibit the surface temperature in each spot. Thermal images and their analysis were obtained with the Thermacam P 2.8 SR – 1 program (Yahav et al., 2005).

determined by the characteristics of the detector array – is used and is found sufficient. Use of a lens with a 24-degree field of view, with the camera placed 60–80 cm from the object resulted in images in which each pixel corresponded to a rectangular detail of 0.9–1.5 mm^2 (see also Section 4.3.4). The IRTI provides accurate measurements of the surface temperature of the whole object; measurements that are undoubtedly more precise and accurate than those provided by thermocouples (Mohler & Heath, 1988).

For birds the actual temperature measured by the IRTI represents the temperature beneath the outer physical surface of the insulating layer. The matrix nature of plumage – which in general lasts for up to 3 weeks on domestic fowl – and of the subsequent feathers causes radiation to be exchanged at varied depths within the outer layer, with the result that the radiative temperature is usually higher than the temperature at the physical surface (McCafferty et al., 2011). Therefore, the IRTI measures the temperature of the feathers/plumage several millimeters below the surface. However, several regions, such as the face, wattle, comb, legs, beak, and unfeathered areas below the wings radiate directly, and their measured temperatures will be those at the surface (Figure 1).

Surface temperature is significantly correlated to the vasomotor responses of the bird. It is well documented that the vasomotor response – vasodilatation or vasoconstriction (Figure 8, for details see Section 4.3.1) is affected by the bird's body temperature (T_b): hyperthermic or hypothermic, respectively (Yahav, 2009).

Birds are endotherms, i.e., they are able to maintain their T_b within a narrow range. In endothermic animals (birds and mammals) T_b is physiologically the most closely controlled parameter of the body, therefore the thermoregulatory system in these animals operates at a very high gain in order to hold T_b within a relatively narrow range, despite moderate to

extreme changes in environmental conditions. The ability to maintain a stable T_b depends on the mechanisms that control heat production and heat loss; mechanisms that changed in the course of evolution, to enable endothermia to replace ectothermia (Silva, 2006). The evolutionary changes from ectothermia to endothermia were achieved because the developmental regulatory mechanisms maintained a balance between heat production and heat loss (Equation 1). Both mechanisms, especially heat production, are probably older than endothermy, but both are permanently activated and regulated by both neuronal and hormonal signals (Morrison et al., 2008; M.P. Richards & Proszkowiec-Weglarz, 2008; Silva, 2006).

Collectively, heat transfer modeling has been used to understand thermoregulation in endotherms in general. These models take into consideration a constant T_b for an animal not performing external work and are represented by the following heat-balance equation, based on the first law of thermodynamics:

$$S = H - E \pm R \pm C \pm K \quad (1)$$

where S is the bodily heat gain or loss that must be balanced by: H metabolic heat production; E evaporative heat loss; R radiative heat gain or loss; C convective heat loss or gain; K conductive heat loss or gain. Body temperature will remain unchanged when S is zero, i.e., heat gain matches heat loss. If more heat is produced and gained than lost, then S is positive and T_b will rise and vice versa (Dawson & Whittow, 2000).

Within equation (1), thermogenesis (heat production - H) can be divided into obligatory and facultative thermogenesis (Silva, 2006). Obligatory thermogenesis refers to the energy required to maintain T_b as long as the ambient temperature (T_a) lies in the thermoneutral zone, the range within which the body is in thermal equilibrium with the environment and produces energy at a level termed the resting metabolic rate (RMR) (Gordon, 1993). Facultative thermogenesis refers to stimulated energy production that is required when T_a deviates below or, to some extent, above the thermoneutral zone. Heat loss – especially with regard to birds, in the present context– is dissipated through respiratory (Marder & Arad, 1989; S.A. Richards, 1968, 1970, 1976; Seymour, 1972) and cutaneous evaporative mechanisms (E) (Ophir et al., 2002; Webster & King, 1987), and sensible heat loss via radiation (R), convection (C) (Yahav et al., 2005) and conduction (K) (Wolfenson et al., 2001).

Because domestic fowl are highly productive their biology causes severe difficulties in coping with changes in the environment, especially with regard to T_a and ventilation. These difficulties, in turn, may lead to severe difficulties in maintaining a dynamic steady state, which can impair productivity. To avoid such deleterious effects, the bird activates evaporative and sensible heat loss mechanisms. However, heat loss via panting is accompanied by loss of body water content, therefore dehydration will reduce heat loss via this pathway, as well as that through extensive passive cutaneous evaporation. Panting is also associated with respiratory alkalosis, which may affect the evaporation (Yahav et al., 1995). An increase in sensible heat loss may reduce the intensity and consequences of evaporative heat loss.

During recent years alterations in incubation temperature (termed "thermal manipulation") have been used to enhance thermotolerance acquisition in the post-hatch fowl (Druyan et al., 2011; reviewed by Yahav et al., 2009). Briefly, thermal manipulation during incubation

aims to change the threshold response of the preoptic anterior hypothalamus (PO/AH) – the principal site in the central nervous system where heat production and heat loss are controlled – in order to elicit appropriate thermoregulatory responses via control of physiological, endocrinological, and behavioral responses and, thereby, to keep the core T_b relatively constant (Boulant, 1996).

To understand the contribution of sensible heat loss to the ability of the domestic fowl to balance the dynamic steady state of its body energy content an IRTI camera had to be used to monitor its body surface temperature, and a special numerical model had to be developed to accurately calculate heat loss by radiation and convection. Furthermore, this technique is used during incubation to determine the effect of incubation temperature on eggshell temperature, and to enhance the effects of these changes on post-hatch thermotolerance acquisition (Piestun et al., 2008, 2009; Shinder et al., 2009).

This Chapter will focus on:

a. The specification of the IRTI camera used for sensible heat loss evaluations; and
b. The sensible heat loss models for domestic fowl (pre- and post-hatch), and their applications.

2. The IRTI camera specifications – Thermal accuracy and calibration

Most infrared cameras that are used for temperature measurements have a guaranteed thermal resolution of 0.1–0.2°C and an absolute accuracy of ± 1–2°C, or 1–2% of the absolute temperature (kelvins, K). This accuracy is not sufficient in biological applications, where

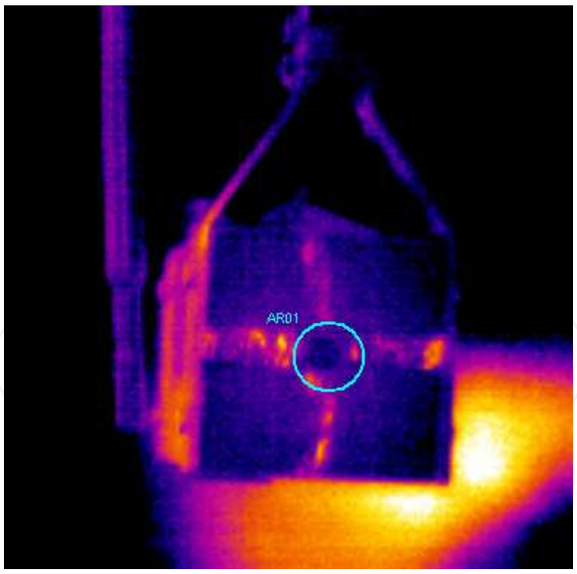

Fig. 2. Infrared thermography of the experimental setup for studying fluctuation of measurements. On the left side, the alcohol thermometer is visible. The blackbody is shown as a box in which the cylinder is confined. The hole of the blackbody cavity appears as a dark area, surrounded by the limits of the ROI (Region of Interest), as defined by the camera software. An electronic temperature probe which measured the actual temperature of the blackbody was inserted into the rear of the cylinder and is invisible to the camera.

comparisons between different thermograms are needed, and the expected temperature changes are, in most cases, smaller than ± 2°C. In order to compensate for differences in the calibration among different thermograms, a common reference point with a known temperature and emissivity must be used. In the studies presented below in this Chapter a simple black body was used (Figure 2); it comprised a closed hollow cylinder with a circular aperture of area about 1 cm^2 in its lid. A high-precision temperature probe connected to a digital thermometer was inserted into the blackbody, and the exact temperature was recorded manually for each thermogram. The blackbody temperature was compared with the camera temperature reading, and the difference between the readings was used to correct the camera readings for each spot in the thermogram. The system was tested also in a commercial chicken farm by comparing simultaneous readings of three temperature measurement systems (Figure 3): 1) a high-precision alcohol thermometer placed in the air; 2) a blackbody with a temperature probe as described above; 3) an IR camera that registered temperature readings for the aperture of the blackbody.

Figure 3 displays typical results of the relation among different measurement systems. During the first 15 minutes, the temperature in the building slowly increased according to the alcohol thermometer which has a shorter equilibration time than the blackbody. After 15

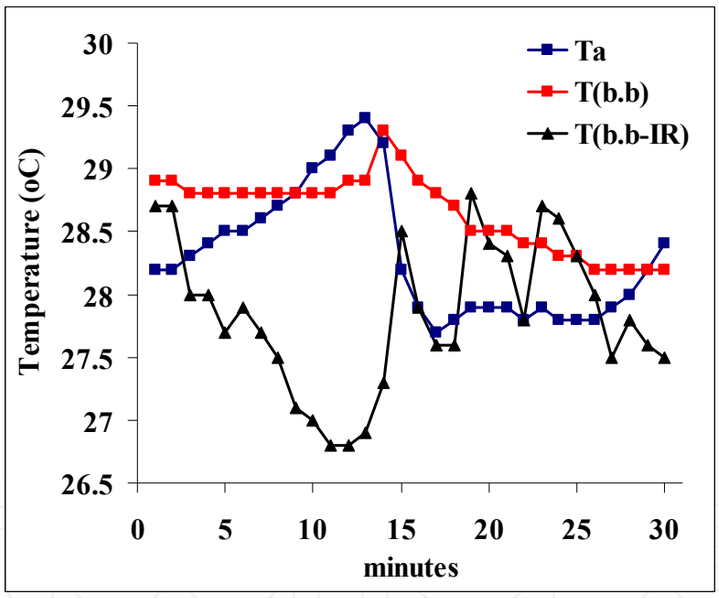

Fig. 3. Comparison between blackbody temperatures measured with a precision digital thermometer, blackbody temperature measured by IR thermography, and ambient temperature measured by a high-precision alcohol thermometer at subsequent instants. A manufacturer-calibrated standard alcohol thermometer was situated 1.5 m above the floor in a commercial poultry house, and the blackbody (described above) was situated immediately adjacent to it. The IR camera was placed 80 cm from the blackbody. The minimum temperature in the hole of the blackbody was measured once a minute, and the digital reading of the blackbody temperature was recorded manually, as was the ambient temperature, as measured by the alcohol thermometer. T(b.b): Digital reading of blackbody temperature; T_a: Ambient temperature, as measured by the alcohol thermometer; T(b.b-IR): Blackbody temperature, as measured by the IR camera.

minutes the ventilation in the farm went on automatically, and the alcohol thermometer displayed an abrupt decline in ambient temperature. The digital thermometer of the blackbody displayed an exponential decline with the same magnitude. During the whole event, before and after the ventilation went on, the absolute blackbody temperature demonstrated both a systematic drift and stochastic fluctuations, displaying errors of up to 2 centigrade. Use of reference temperature measurements implies that each thermogram analysis is based on three measured inputs: the camera reading of the measured spot or the ROI, the camera reading of the blackbody temperature, and the digital reading of the blackbody temperature. In light of the uncertainty of equilibration, the effect of changes in the environment on the camera readings, and the intrinsic fluctuation in each of the inputs, one can hardly expect that using a reference point could eliminate stochastic fluctuations in the measurements. However, systematic drift in the camera calibration can be compensated for accurately.

Figure 4 illustrates the setup for field measurements; it enabled the blackbody to be kept in focus in all thermograms. Figure 5 shows the experimental setup in the laboratory, and Figure 6 shows a typical thermogram produced in the laboratory; the blackbody is clearly distinguishable. The camera reading of the blackbody temperature was obtained by means of an automatic feature that enabled display of the minimal temperature if the blackbody was colder than the surroundings in the region of interest (ROI), or the maximal temperature if it was warmer. However, in some cases the aperture was not distinguishable in the thermogram because the temperature differences in the region were too small, i.e., if the difference between maximum and minimum temperatures in the ROI was less than 0.5°C. In such cases the average temperature of the ROI was used, thus allowing for a

Fig. 4. Setting of field observations. The camera was attached in a permanent position at one end of a special "antenna", and the blackbody was situated at the other end, with the hole facing the camera. The distance between the lens and the blackbody was 80 cm. At the right-hand side of the picture can be seen the wire that connected a temperature probe that was inserted into the rear of the blackbody to the digital thermometer, which is displayed in front of the camera only for this photograph. During experimental measurements this thermometer was carried in a small bag, and the digital blackbody temperature was recorded manually for each thermogram.

Fig. 5. Experimental procedure in the laboratory. The setting was identically arranged and located in each of the four climate-controlled rooms in which birds were exposed to various environmental conditions. The IR camera was permanently placed 80 cm from the blackbody.

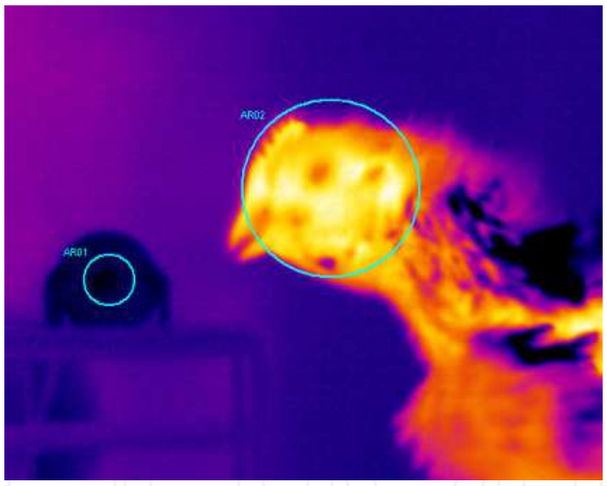

Fig. 6. Typical thermogram obtained in laboratory measurements. Two regions of interest were used for the analysis: one around the hole of the blackbody and the other around the hotter parts of the chicken's face. Camera software was used to read the minimal temperature of the blackbody cavity if it was colder than the surrounding, its maximal temperature if it was hotter than the surrounding, and its average temperature if the cavity was indistinguishable on the thermogram because the temperature differences were too small. For facial temperature measurement, the hottest temperature inside the ROI surrounding the face was recorded.

maximum error of 0.3°C. Since this occurred in a relatively small number of thermograms, the effect on averages of several thermograms was estimated to be not greater than 0.1–0.2°C, which was not crucial in this application.

3. Sensible heat loss from fertile eggs of domestic fowl – The rationale, the model and the applications

3.1 The rationale

During the perinatal period, a time window occurs in which physiological control systems can be imprinted. This imprinting is probably related to neural changes at the microstructural level, i.e., in terms of synaptic plasticity, as well as by environment-induced modifications of gene expression. Perinatal epigenetic temperature adaptation may be used as a tool to adapt poultry embryos or hatchlings to subsequent climatic conditions (Tzschentke, 2007; Tzschentke & Plagemann, 2006). In chickens and other precocial birds, epigenetic temperature adaptation can be induced by changes in incubation temperature during late-stage embryonic development (Collin et al., 2007; Minne & Decuypere, 1984; Piestun et al., 2009; Shinder et al., 2009; Tzschentke & Halle, 2009; Tzschentke & Nichelmann, 1997), as well as by post-hatch thermal conditioning (Yahav & Hurwitz, 1996; Shinder et al., 2002). To calculate heat loss by radiation and convection from fertile eggs a specific model was developed.

3.2 The model

Sensible heat loss from fertile eggs can be calculated according to van Brecht et al. (2005) and Shinder et al. (2007), on the assumption that heat exchange occurs via the whole eggshell surface. The eggshell surface area is determined from the length and breadth of the egg, which, for the purpose of the following model were measured with calipers (Mitutoyo-Ser. No 51015023; precision, 0.02 mm; Mitutoyo Corporation, Kanagawa, Japan). The egg was assigned a characteristic dimension, i.e., the diameter of a sphere with the same surface area (van Brecht et al., 2005).

The very low air velocity (less than 0.3 m s^{-1}) to which the eggs were exposed necessitated the use of a theoretical heat transfer model based on free convection and radiation. The spherical-egg model, incorporating mean values of available or especially derived heat-transfer correlations, was used to calculate the sensible heat loss (Shinder et al., 2007).

The exponential dynamics of cooling following an abrupt decrease in T_a (Tazawa & Nakagawa, 1985; Tazawa et al., 2001) was fitted to the exponential equation:

$$T_{egg}(t) = T_1 + A \exp(-k\,t) \quad (2)$$

where T_{egg} is the eggshell temperature as measured by IRTI; T_1 is the extrapolated asymptotic temperature as $t \rightarrow \infty$, which may differ from T_a during cold exposure; $T_1 + A$ is the extrapolated temperature at the moment of onset of the cold exposure ($t = 0$); The decay-rate or cooling-rate coefficient, k is the reciprocal of the time constant, t_1, and is related to the thermal half-time, $t_{1/2}$ (min) according to:

$$k = 0.693 / t_{1/2} \quad (3)$$

The estimated total accumulated heat loss (measured in units of energy) from the egg during its cold exposure may be a physiologically relevant measure of the intensity of the cold exposure, and it can be calculated from T_{egg}, as measured by IR thermography. Since the total heat content of the egg is proportional to T_{egg}, the instantaneous value of SHL, q

(watt) is proportional to dT_{egg}/dt, which has the same decay rate, k, as T_{egg}. After the abrupt reduction of T_a, q can, therefore, be fitted into an exponential decay curve described by:

$$q = q_0 + q_1 \bullet \exp(-kt) \quad (4)$$

where q_0 is the extrapolated value at large t, when the living embryo is in quasi-equilibrium with the environment. The extrapolated heat loss at t = 0 is $q_0 + q_1$. The decay rate k [min^{-1}] is as described above. The initial heat loss per degree of temperature change, in watt/^oC was designated as G:

$$G = (q_0 + q_1)/\Delta T \quad (5)$$

where ΔT is the initial difference between T_{egg} and T_a. To calculate G, the incubation temperature was used instead of T_{egg}, because the differences between the two parameters could be neglected within the accuracy of the overall calculation.

Disregarding the asymptotic "plateau" q_0, which represents the metabolic heat production of the embryo, the total sensible heat loss (Q) caused by a cold exposure for Δt min will be:

$$Q = \int_0^{\Delta t} (q - q_0) \bullet dt = (q_1/k) \bullet (1 - \exp\{-k \bullet \Delta t\}) \bullet 60/4.19 \quad (6)$$

where Q = total accumulated heat loss (Calories); q = instantaneous rate of heat loss (watt); k = decay rate (min^{-1}).

The parameter Q in Equation (6) represents a quantitative estimate of the total physiological impact of the cold exposure, and it can serve as a suitable indicator for comparing different temperature manipulation strategies.

3.3 The applications

Short-term cold exposure during the late phase of embryogenesis, when embryos switch from ecto- to endothermic behavior, was found to induce an enhanced thermogenesis pattern in the hatched chicks (Minne & Decuypere, 1984; Nichelmann, 2004).

In order to study the effect of reducing incubation temperature during the final phase of embryogenesis on thermotolerance acquisition of post-hatch chicks, embryos were exposed to 15°C for 30 or 60 min on embryogenesis days 18 and 19. IRTI was used to measure the eggshell surface temperature, to determine sensible heat loss from the egg during 60 min of cold exposure (Figure 7), in order to determine its effect on post-hatch parameters (Shinder et al., 2009).

Figure 7 depicts the calculated time variation of SHL from the eggs, obtained by fitting the data to an exponential-decay regression curve according to Equation (4). The calculated q_0 was 0.55 ± 0.14 W; q_1 was 1.81 ± 0.11 W; and k was 0.032 ± 0.006 min^{-1}. Eggs exposed to 15°C for 60 min exhibited decreases in temperature and in SHL with a high degree of correlation with the regression curve (R^2 = 0.98). The calculated G was 0.1 ± 0.01 W/°C (Equation 4). The total SHL from eggs, according to Equation 6, with the extreme values of q_1 and k were 512 ± 66 and 718 ± 126 cal for cold exposures of 30 and 60 min, respectively. These findings are of great importance in the application of cooling of fertile eggs during incubation.

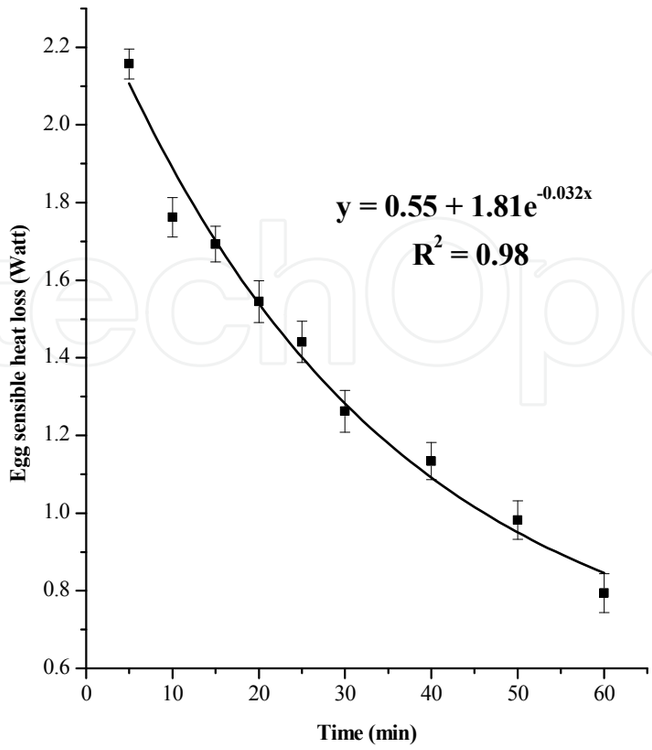

Fig. 7. Sensible heat loss from eggs by convection and radiation during 60 min of cold exposure (15°C) on d 19 of incubation (E19), fitted to an exponential regression curve (Mean ± SE; n = 8; P < 0.05) (According to Shinder et al., 2009).

4. Convective and radiative heat transfer from fowls: Heat transfer relationships – The rationale, the model and the applications

4.1 The rationale

It has been assumed that sensible heat loss does not play an important role in the domestic fowl when T_a is above the upper boundary of the thermoneutral zone (for review see Hillman et al., 1985). This assumption was based on: a. the small difference between the body surface temperature (T_s) and T_a; and b. the fact that in fully feathered birds only limited areas are unfeathered, i.e., legs, head, wattle and comb. However, use of the IRTI camera for non-invasive surface-temperature measurements has shown that sensible heat loss can amount to approximately 45% of the total heat loss under specific environmental conditions (Yahav et al., 2004) and thus can reduce the deleterious effects of panting.

4.2 The model (according to Yahav et al., 2005)

To calculate heat transfer from the fowl, each part of the surface is represented by a corresponding geometrical shape. For each part, radiative and convective heat transfers are estimated by means of available and especially developed heat transfer relationships. Below is a short introduction on convective and radiative heat transfer, followed by a detailed discussion on the relationships used.

4.2.1 Convective heat transfer

Heat is transferred by convection when a body at a given temperature is in contact with air at another temperature. The convective heat flux, q_c, depends on the temperature difference ΔT, between the body and the air, the area of contact A, and the heat-transfer coefficient h:

$$q_c = hA\Delta T \tag{7}$$

The average heat transfer coefficient, h, depends on the geometry of the body, the physical properties of the air and the flow regime. The major difficulty in calculating q_c stems from the strong dependence of h on the flow regime.

The heat transfer coefficient, h, is expressed through the nondimensional group known as the Nusselt number:

$$Nu = \frac{hD}{k} \tag{8}$$

where D is the body length scale, e.g., diameter in the case of a sphere or a cylinder, and k is the thermal conductivity of the air. Heat-transfer relationships given in the literature relate the Nusselt number to two other nondimensional groups. The first is the Reynolds number:

$$Re = \frac{UD}{\nu} \tag{9}$$

where U is the air velocity and ν is the kinematic viscosity. The second is the Prandtl number:

$$Pr = \frac{\nu}{\kappa} \tag{10}$$

where κ is the thermal diffusivity of the air. The three groups are related, in general, by:

$$Nu = f(Pr, Re) \tag{11}$$

where the function f is specific to each geometry and flow regime.

Below we present, for each part of the fowl surface, the appropriate relationship in the form of Eq. (11). This enables calculation of h and heat transfer for each part by using Eq. (7) and thence the total convective heat transfer from the bird.

4.2.2 Radiative heat transfer

Heat transfer by radiation occurs through electromagnetic radiation from one surface to another because of the temperature difference between them. The rate of radiative heat transfer between two surfaces depends on their temperatures, the view area, and the respective surface emissivities.

Radiative heat transfer between the fowl and its environment and among adjacent organs, e.g., the two legs, of the fowl itself occurs if temperatures are different. The view area changes frequently because of movement of the bird. In our model it is assumed that

radiative heat transfer takes place only between the fowl and its environment, and we neglect radiation among the bird's surface parts. We also treat the environment as a large surface at uniform temperature that surrounds the relatively small bird.

Radiative heat flux from (or to) the animal is estimated as:

$$q_r = \varepsilon_1 \sigma A_1 (T_1^4 - T_2^4) \tag{12}$$

where subscript *r* stands for radiation, indices 1 and 2 represent, respectively, the body surface and the environment, ε (= 0.96) is the emissivity of a biological tissue, σ is the Stefan-Boltzmann constant (= 5.669×10^{-8} $Wm^{-2}K^{-4}$), *A* is the surface area and *T* is the absolute temperature.

4.2.3 Convective heat transfer from different parts of the bird surface

The present simple model is based on the following two assumptions:

- The bird is at rest, facing the upstream airflow direction. In practice the bird is frequently in motion, but this is not considered in the model.
- Heat transfer is by forced convection because the wind speed is rarely low enough for free convection to occur. This was validated for the air speeds associated with the present study.

The IR thermal imaging system measured the surface temperature of each surface part as well as the ambient temperature. The areas of the surface parts also were estimated from the thermal images. As mentioned above, to estimate the heat transfer by convection, the coefficient *h* was estimated for each surface part by using the following relationships:

The comb was simulated as a rectangular flat plate exposed to uniform flow parallel to its long side. The corresponding heat-transfer relationship was that for forced convection from a flat plate. According to the experimental air speed and dimensions of the comb the flow was laminar, therefore (Holman, 1989):

$$Nu = 0.664 Re^{1/2} Pr^{1/3} \tag{13}$$

where the length scale of the nondimensional parameters Re and Nu is the comb length. The heat-transfer coefficient is calculated by using Eqs. (8) and (13), and the convective heat transfer is estimated by using Eq. (7) where *A* is the total area of the two sides of the comb, taken as two equal rectangular surfaces.

Each wattle is modeled as a circular flat plate immersed in a uniform flow parallel to its surface. Our literature search for a relationship for such a configuration was unsuccessful. Therefore the required relationship was derived from that for a rectangular flat plate (Eq. (13) above). In particular, the surface of the circular plate was simulated as an infinite number of narrow rectangular plates, each of different length. For each thin plate Eq. (13) was applied and the average heat transfer coefficient over the circular plate was obtained by integration:

$$Nu = 0.7389 Re^{1/2} Pr^{1/3} \tag{14}$$

The characteristic length scale was the wattle diameter and the area was the total for four sides of the two wattles.

The bird's face is modeled the same way as the wattles, i.e., as a flat circular surface exposed to a parallel uniform airflow. Thus Eq. (14) is applied, with the effective area being the two sides of the face. In some adult birds it was evident that each face surface was closer to a semicircle than a full one: in these cases, the same relationship was used (i.e., Eq. (14)) with the adjusted heat transfer area applied in Eq. (7).

The leg is modeled as a circular cylinder in uniform cross flow. Many empirical heat transfer relationships for this configuration can be found in the literature. In the one chosen here, the relationship depends on the value of Re (Holman, 1989):

$$\mathrm{Nu} = (0.43 + 0.5\,\mathrm{Re}^{1/2})\,\mathrm{Pr}^{0.38} \qquad (\text{for } 1 < \mathrm{Re} < 1000) \tag{15}$$

$$\mathrm{Nu} = 0.25\,\mathrm{Re}^{0.6}\,\mathrm{Pr}^{0.38} \qquad (\text{for } 1000 < \mathrm{Re} < 200{,}000) \tag{16}$$

The length scale in the expressions for Nu and Re is the diameter of the extremity and the area is its surface area.

The toes are also modeled as circular cylinders in uniform cross flow. We assume that for all toes the flow is perpendicular to the cylinder axis. Therefore Eq. (15) or (16) is applied but, because of the small diameter of the toes, and the consequently small Reynolds number, Eq. (15) was usually used. In calculating the heat flux, eight equal-area toes were assumed, although in practice the toes' areas are not identical.

The bird's neck also is modeled as a cylinder in a uniform cross flow. The heat-transfer coefficient is calculated by using either Eq. (15) or Eq. (16), depending on the value of Re.

The body of the fowl is modeled as a sphere immersed in a uniform flow. We assume that the limbs are always in contact with the body, although sometimes they are not; the effect of separated wings is discussed below. The relationship for air at room temperature (Pr = 0.71) is given by Holman (1989):

$$\mathrm{Nu} = 2 + (0.25 + 3\times10^{-4}\,\mathrm{Re}^{1.6})^{1/2} \qquad (\text{for } 100 < \mathrm{Re} < 300{,}000) \tag{17}$$

The bird separates its **wings** from its body under extremely warm conditions, thus forming two channels through which airflow enhances cooling. Assuming that the two channels are rectangular, we apply the Petukhov equation (Ozisik, 1985):

$$\mathrm{Nu} = \frac{\mathrm{Re}\,\mathrm{Pr}}{8\mathrm{X}}\mathrm{f} \qquad (\text{for } 10^4 < \mathrm{Re} < 5 \times 10^6) \tag{18}$$

where

$$\mathrm{X} = 1.07 + 12.7(\mathrm{Pr}^{2/3} - 1)\left(\frac{\mathrm{f}}{8}\right)^{1/2} \tag{19}$$

and f is the friction factor (= 0.07) which can be evaluated from the Moody diagram. The Reynolds number is based on the hydraulic diameter, $\mathrm{D_h} = 4\mathrm{A_c} / \mathrm{P}$, in which A_c is the cross-

sectional area of the duct and P is its perimeter. The airspeed substituted in Re was half the ambient air speed surrounding the bird. This roughly accounted for the reduction in air speed caused by the high frictional surface of the wing. The resulting $Re \approx 3 \times 10^3$, is smaller than the lower validity limit of Eq. (12). Nevertheless this equation was used in the model to provide a rough estimate of the convective heat flux through the wing channels.

4.2.4 Radiative heat transfer from different parts of the body surface

In using the above assumptions, each part of the body surface is considered to be a small body surrounded by a large, uniform-temperature environment. The radiative heat flux is calculated by using Eq. (12) with A_1 as the surface area of the body part. It is assumed that there is no radiative heat transfer associated with the channels formed by the separated legs.

4.3 The applications

The vasomotor response of the peripheral blood system that result from changes in environmental conditions (temperature, ventilation, relative humidity) can be evaluated non-invasively by IRTI. The vasomotor response immediately affects skin temperature, which increases or decreases as a result of vasodilation or vasoconstriction, respectively. In many biological studies the effects of various treatments on vasomotor responses is of great importance, both scientifically and practically. These two aspects are discussed below.

4.3.1 Evaluating vasomotor response in domestic fowl: Vasoconstriction vs vasodilation

The epigenetic temperature adaptation approach is based on the hypothesis that thermal manipulations during embryogenesis may affect the PO/AH threshold for heat loss, i.e., they may affect heat loss by radiation and convection; in other words, they may change the vasomotor response.

Based on this hypothesis, Piestun et al. (2008, 2009), elevated the incubation temperature between embryogenesis (E) days E7 to E16 for 12 h/d (12H) or continuously (24H) to establish a better post-hatch vasodilatation response of the peripheral blood system.

This phenomenon could be evaluated by measuring the temperatures of the chicken surface and of its surroundings (Figure 8). This information was used to calculate sensible heat loss and indirectly to determine the vasomotor efficacy.

Figure 8 illustrates the efficacy of the vasomotor response of those chickens that had been thermally manipulated during embryogenesis. Under both high and relatively low T_a conditions the manipulated broilers exhibited significantly better vasodilatation (35°C) or vasoconstriction (23°C) than controls, as highlighted by the significantly higher and lower heat losses at the low and high T_a, respectively.

4.3.2 Correlation between body temperature and facial surface temperature

The commonly used ways to measure T_b are invasive and time consuming and, therefore, may be traumatic, affecting T_b within a few minutes (Cabanac & Aizawa, 2000; Cabanac & Guillemette, 2001), but the adoption of IRTI in biological sciences has enabled non-invasive, non-contact measurement of surface temperature.

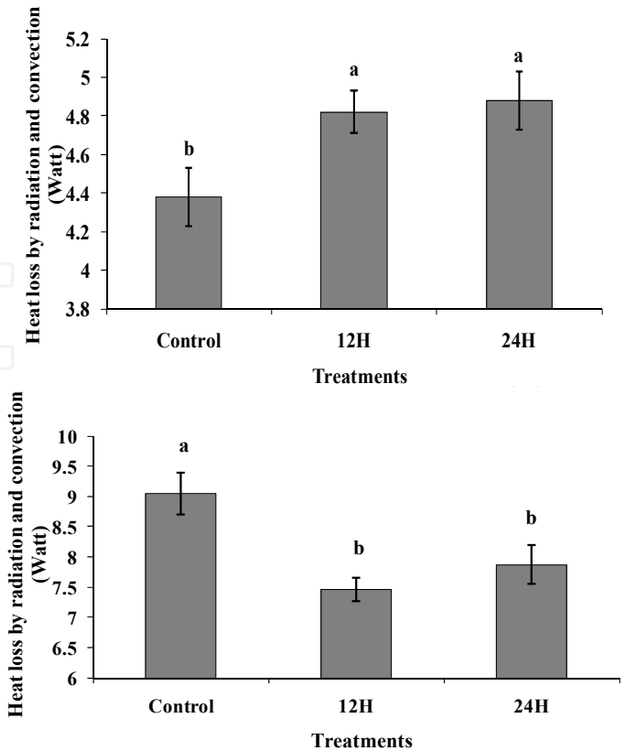

Fig. 8. The effects of two different ambient temperatures (35°C – upper; 23°C – lower) on heat loss by radiation and convection from broiler chickens that had been thermally manipulated during embryogenesis (embryogenesis days 7 to 16) for 12 h/d –12H – or continuously – 24H – in order to change their vasomotor responses.

However, use of IRT measurement of skin surface temperature in monitoring the thermal status of chickens in a commercial flock necessitates selection of a specific surface site, and determination of the exact correlation of its temperature with T_b under various environmental conditions. A reliable correlation between facial surface temperature and T_b could shed light on the thermal-physiological status of the organism. This application, in which facial surface temperature measured by IRTI can serve as an important indicator of the thermal-physiological status of the fowl, could dramatically improve poultry house environmental control by adapting it to the needs of the client – the domestic fowl.

Thermographic imaging in poultry breeding can be relevant only if a satisfactory correlation exists between the chickens' body temperature and facial surface temperature. Our studies demonstrated that such a correlation can indeed be found. In the laboratory, where the climatic conditions were relatively similar for all the chickens, individual body temperatures correlated well with individual facial surface temperatures for chickens that were exposed to acute environmental heat conditions, both with and without ventilation, and to persistent heat without ventilation (Figure 9). Moreover, if a distinction was made between acute and persistent heat exposure, body and facial temperatures correlated remarkably better than ambient temperature with hormonal stress symptoms (Figure 10).

The hormonal analysis was crucial for correlating temperature data with the changes in the physiological status of the chicken that resulted from exposure to acute or persistent heat.

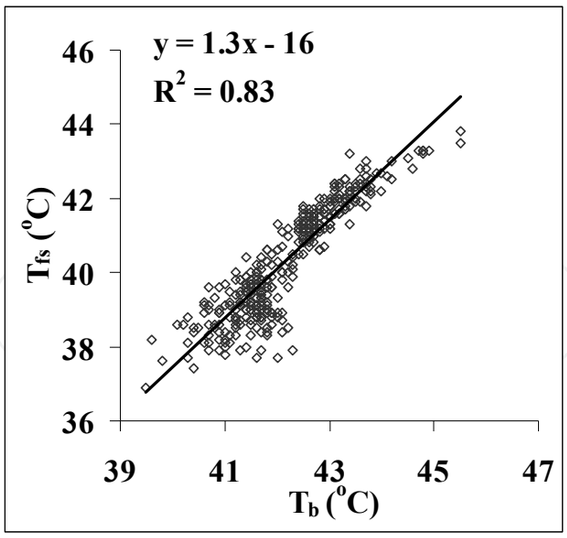

Fig. 9. Correlation of individual Facial Temperature (T_{fs}) with Body Temperature (T_b). Chickens were reared under controlled conditions, and on each of days 8, 15, 22, 29 and 36 a group was randomly chosen for exposure to three different heat treatments: acute heat only; acute heat together with ventilation; and persistent heat. In each treatment 27 chickens were used: 18 chickens in each treatment were used for measuring the response of hormone concentrations to the treatments; the remaining nine were used to monitor the responses of body and facial temperatures. The data presented in the graph are for all measurements of individual chickens in all treatments and of all ages. The linear regression curve is a least-squares curve calculated by Excel.

Four major hormones were selected: thyroxin (T_4), triiodothyronine (T_3), corticosterone and arginine vasotocine (AVT). The first two of these relate directly to the metabolic status of the chicken, whereas corticosterone is a well known indicator for stress level, and AVT for hydration status.

The correlations of the plasma concentrations of T_4 and T_3 with body, facial surface and ambient temperature during persistent exposure to heat are presented in Figure 10, as examples. Table 1 summarizes the statistical analysis and the R^2 values for correlations between T_4, T_3, corticosterone and AVT concentrations and the various temperature parameters – body, facial and ambient. In acute treatments, with or without ventilation, the corticosterone concentration displayed a statistically significant positive correlation and triiodothyronine a significant negative correlation with body and facial temperature ($p < 0.05$), whereas the regression with ambient temperature was not significant. The responses of these hormones were found to be consistent with previously described physiological reactions to acute heat stress (Darras et al., 1996; Iqbal et al., 1990).

During exposure to persistent heat, significant negative regressions were found for the correlations of T_4 and T_3 with body and facial temperatures. Only T_3 displayed a significant regression with ambient temperature also, although this regression was somewhat weaker (R^2 lower) than that with physiological temperatures. AVT showed a strong negative correlation with facial temperature, a weaker correlation with ambient temperature, and no correlation with body temperature.

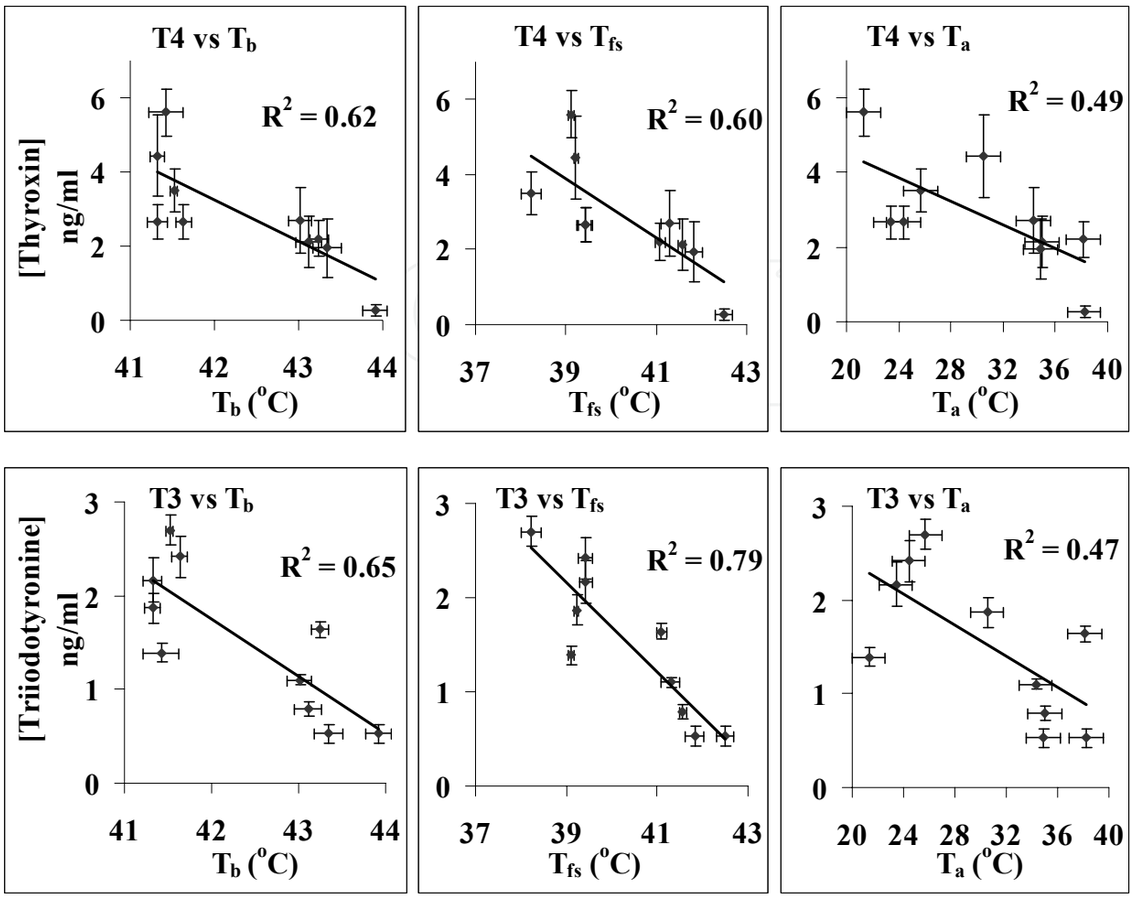

Fig. 10. Correlation of blood plasma concentrations of thyroid hormones – Thyroxine (T_4) and Triiodothyronine (T_3) – with three different temperature parameters during persistent exposure to heat. Data are from the experiment described in the legend to Figure 8. Each data point represents the average for one group of chickens aged between 7 and 35 days, during one measurement (n = 9). T_4, Thyroxin; T_3, Triiodothyronine; T_b, Body temperature; T_{fs}, Facial Surface temperature as measured with IRTI; T_a, Ambient temperature. The linear regression curves are least-squares curves calculated by Excel. Error bars are ± s.e.

One can conclude from the above results that in the laboratory setting facial temperature, as measured by thermographic imaging was more closely related than the ambient temperature to parameters that indicate the birds' thermal and stress status. It further can be concluded that the high positive correlation between facial and body temperature can be exploited commercially to detect thermal stress in the birds without use of invasive measurements.

4.3.3 Field observations

In commercial poultry houses it is well-known that environmental conditions are far from homogenous, even when a building is equipped with a climate-control system. It was therefore not surprising that in field studies the variation in the correlation between T_b and facial surface temperature was larger than in the laboratory. However, even for individual

		Chronic heat			Acute heat		
		T_b	T_{fs}	T_a	T_b	T_{fs}	T_a
Corticosterone	R^2	0.01	0.00	0.07	0.33	0.29	0.12
	p	0.79	0.97	0.49	**0.03**	**0.04**	0.21
Thyroxin	R^2	**0.62**	**0.60**	0.49	0.05	0.05	0.07
	p	**0.02**	**0.02**	0.06	0.34	0.35	0.26
Triiodothyronine	R^2	**0.65**	**0.79**	0.47	0.34	0.40	0.17
	p	**0.00**	**0.00**	**0.03**	**0.02**	**0.01**	0.13
Arginine vasotocin	R^2	0.36	**0.51**	0.16	0.01	0.05	0.02
	p	0.06	**0.02**	**0.03**	0.72	0.43	0.65

R^2 values larger than 0.50 and *p* values smaller than 0.05 are printed in bold.

Table 1. R^2 values, and significance probability (*p*) for the correlations of average hormone concentrations with body temperature (T_b), facial surface temperature (T_{fs}), and ambient temperature (T_a).

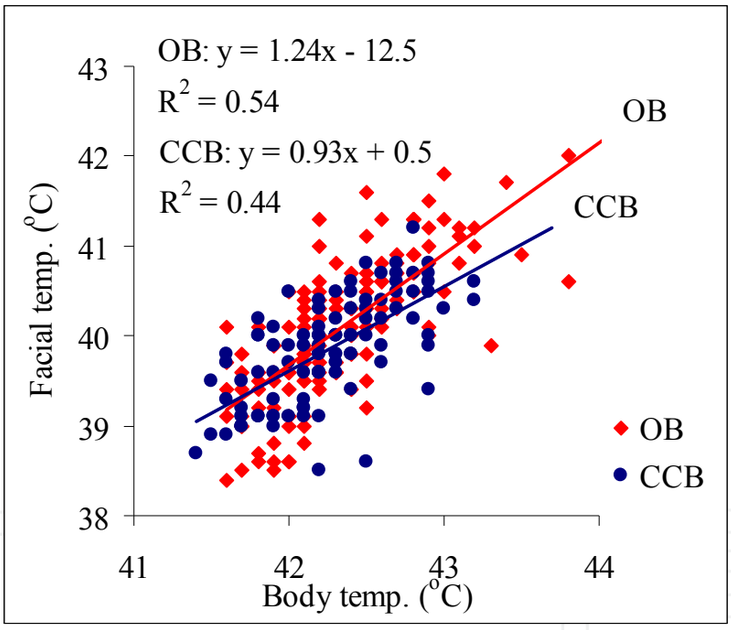

Fig. 11. Correlation between individual body and facial temperatures in two commercial buildings. Two commercial poultry flocks in Kibbutz Lavi were monitored during 36 h. The flocks were in two different buildings: a closed climate-controlled building (CCB) and an open building (OB). Measurements were performed in "stations" in which 50–70 randomly selected chickens were confined in a detachable cage, and were then immediately caught one by one, and their body and facial temperatures were measured simultaneously. When behavioral stress became evident the procedure was interrupted, generally after 10–20 chickens had been measured. Three measuring sessions were performed: starting at midday when the chickens were 30 days old, the following midnight, and the following midday. In each measuring session three to five stations were surveyed in each flock.

chickens a certain correlation was found in the field measurements (Figure 11). The correlation between the two temperatures (face and body) was clearly revealed when averages of facial temperature for each "measurements station" were plotted against the corresponding average of T_b (Figure 12). Although an average of only 15 chickens were recorded for body and facial temperatures in each station, a strong linear regression could be drawn between the averages.

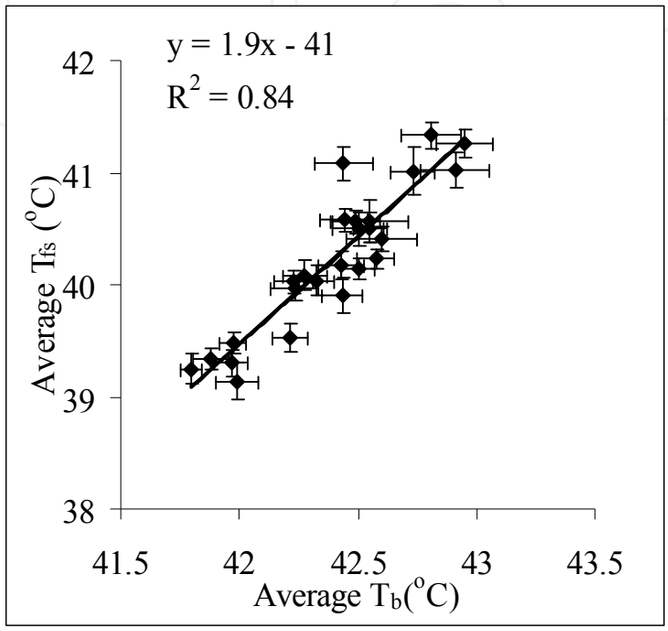

Fig. 12. Correlation between sub-population averages of body and facial temperatures in two commercial buildings. The experiment is described in the legend to Figure 11. Data are averages of body and facial temperatures that were calculated for each measuring station under identical environmental conditions. Regression for both of the buildings together is displayed. Error bars are ± s.e.

4.3.4 The possibility of reducing costs by using low spatial resolution

The algorithm discussed in this Chapter – for calculating the facial temperature of chickens from the thermal data of a thermographic image – was based on locating the maximal temperature within a manually defined circular region of interest (ROI) that comprised the relatively unfeathered area around the ear and eye on the chicken's face. This temperature – termed the "hottest spot temperature" – was preferred over the calculated average temperature of the chicken's face because of ambiguity in defining the face. However, the notion of a "spot" is misleading because of the limited spatial resolution of the images. The camera was equipped with a sensor array of 320 × 240 pixels. Using a lens with a 24-degree field of view, and placing the camera 60–80 cm from the object (chicken) resulted in images in which each pixel corresponded to a rectangular area of 0.9–1.5 mm^2. The "hottest spot" is therefore equivalent to the one among an array of such areas that had the highest average temperature.

Analysis of the economic feasibility of hypothetical commercial applications of IRTI in poultry breeding clearly showed that including IR cameras that cost tens of thousands of

American dollars in a flock-monitoring system was not a realistic option. It was therefore clear that for commercial applications one must compromise in spatial resolution, which today is one of the main factors that determine the prices of cameras. The question is, therefore: What is the smallest detail that has to be identified in a thermographic image in order to maintain the strong correlation between "hottest spot" temperature and body temperature? In order to check the sensitivity of this correlation to spatial resolution we re-analyzed a few experiments, simulating the "hottest spot" algorithm for the same images with lower spatial resolution. An array of rectangular ROIs was created in the image, to represent part of a (44 × 40)-pixel array, within the (320 × 240)-pixel field of view of the camera. In this configuration each pixel corresponded to about 34 mm² for an object located 60 cm from the camera.

The average temperature of each region of interest was listed, and the highest average was chosen as a "low-resolution hottest spot" temperature. Facial temperatures determined in this low-resolution algorithm and those determined with the high-resolution algorithm were then plotted against body temperature (Figure 13). As expected, low-resolution "hottest spot" temperatures were somewhat lower than high-resolution "hot spot" temperatures because, in the low-resolution configuration peak temperatures were blurred by averaging over a larger area.

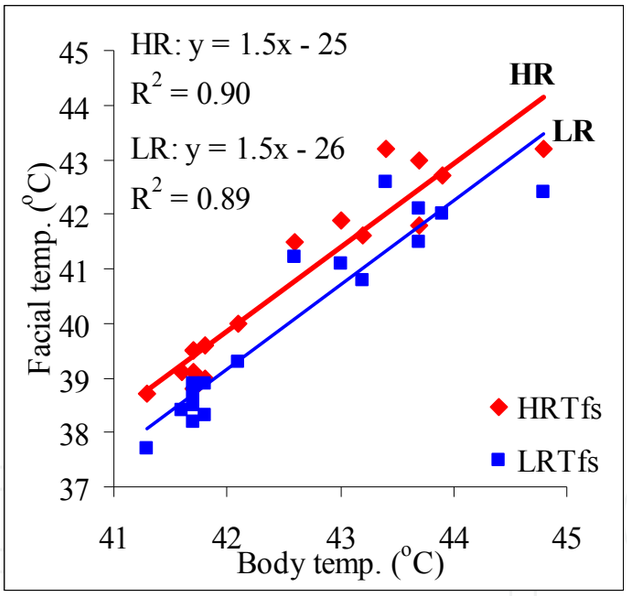

Fig. 13. Typical experimental correlation between facial temperature and body temperature, calculated with a high-resolution algorithm (320 × 240 pixels) and a low-resolution algorithm (40 × 44 pixels). HR, High resolution; LR, Low resolution; Tfs, facial temperature. Regression lines are least squares fit linear regressions computed with Excel.

However, surprisingly, the regression (R^2) between T_b and facial surface temperature was not sensitive to spatial resolution. In the example shown in Figure 13 R^2 values were practically identical: 0.90 for high resolution and 0.89 for low resolution. Three other experiments were analyzed in this cumbersome way, with similar results (not shown). One can conclude that future commercial applications of IRTI in poultry breeding will be able to

use low-resolution equipment, thereby reducing costs significantly without impairing the accuracy of the results.

5. Overall conclusions

- The IRTI camera is an efficient and accurate means of measuring the body surface temperature of domestic fowl as a basis for calculating heat loss by radiation and convection and for evaluating the vasomotor response of fowl subjected to varied environmental conditions.
- This technique enables determination of the rate of heat loss from a fertile egg during thermal manipulations that impart epigenetic temperature adaptation to the manipulated embryo.
- Use of The IRTI technique facilitates the correlation between body temperature and facial surface temperature to assess the physiological status of the chicken under laboratory or commercial environmental conditions.
- The possibility to assess changes in the thermal status of a commercial flock through non-contact measurements can potentially be utilized for improving climate-control systems and spotting situations of acute thermal stress.
- Future commercial applications of this technique could, therefore, contribute to improving both performance and welfare of the flock, and thereby enable the poultry industry to meet future challenges posed by global climate change and the need for cheap sources of meat for the world's growing population.

6. Acknowledgements

Thanks are due to: Dmitry Shinder, The Volcani Center for technical assistance; Jens Vogt, Infratec, Dresden, Germany, for advice and guidance during the initial stages of the project; the teams of RDT and Asio Vision, Tel-Aviv, Israel, for generously lending equipment when needed; and the poultry breeding team in Kibbutz Lavi, Israel, for assisting with observations in the commercial farm.

7. References

Boulant, J. A. (1996). Hypothalamic neurons regulating body temperature, In: *Handbook of Physiology*. Section 4: Environmental physiology. Fregly, M. J. & Blatteis, C. M. Eds.), pp. 105-126. APS, Oxford University Press, New York.

Cabanac, M. & Aizawa, S. (2000). Fever and tachycardia in a bird (*Gallus domesticus*) after simple handling. *Physiol. Behav.,* Vol. 69, pp. 541–545.

Cabanac, A. J. & Guillemette, M. (2001). Temperature and heart rate as stress indicators of handled common eider. *Physiol. Behav.*, Vol. 74, pp. 475– 479.

Cetingul, M. P. & Herman, C. (2010). A heat transfer model of skin tissue for the detection of lesions: sensitivity analysis. *Phys. Med. Biol.*, Vol. 55, pp. 5933–5951.

Chiu, W. T., Lin, P. W., Chiou, H. Y., Lee, W. S., Lee, C. N., Yang, Y. Y., Lee, H. M., Hsieh, M. S., Hu, C. J., Ho, Y. S., Deng, W. P. & Hsu, C. Y. (2005). Infrared thermography to mass-screen suspected SARS patients with fever. *Asia Pac. J. Public Health*, Vol. 17, pp. 26-28.

Collin, A., Berri, C., Tesseraud, S., Rodón, F. E., Skiba-Cassy, S., Crochet, S., Duclos, M. J., Rideau, N., Tona, K., Buyse, J., Bruggeman, V., Decuypere, E., Picard, M. & Yahav, S. (2007). Effects of thermal manipulation during early and late embryogenesis on thermotolerance and breast muscle characteristics in broiler chickens. *Poultry Science*, Vol. 86, pp. 795–800.

Darras, V. M., Kotanen, S. P., Geris, K. L., Berghman, L. R. & Kühn, E. R. (1996). Plasma thyroid hormone levels and iodothyronine deiodinase activity following an acute glucocorticoid challenge in embryonic compared with posthatch chickens. *Gen. Comp. Endocrinol.*, Vol. 104, pp. 203–212.

Dawson, W. R. & Whittow, G. C. (2000). Regulation in body temperature, In: *Sturkie Avian Physiology*. Whittow, G. C. (Ed.). pp. 343-390. Academic Press, San Diego, CA, USA.

Druyan, S., Piestun, Y. & Yahav, S. (2011). Heat stress in domestic fowl – genetic and physiological aspects, In: *Body Temperature Control*. Cisneros, A. B. & Goins, B. L. (Eds.) Nova Science Publishers Inc. New York (in press).

FLIR Systems (2004). *ThermaCAM P65 Operators Manual*. FLIR Systems Publications Vol. 1, pp. 557–954.

Gordon, C. J. (1993). *Temperature Regulation in Laboratory Rodents*, New York, Cambridge University Press.

Hammel, H. T. (1956). Infrared emissivities of some arctic fauna. *J. Mammal.*, Vol. 37, pp. 375–378.

Herman, C. & Cetingul, M. P. (2011). Quantitative visualization of skin cancer using dynamic thermal imaging. *J. Vis. Exp.*, Vol. 5, p. 2679 (abstract).

Hillman, P. E., Scott, N. R. & Van Tienhoven, A. (1985). Physiological responses and adaptations to hot and cold environments, In: Stress *Physiology in Livestock* Yousef, M. K. (Ed.), pp. 27-71, CRC Press, Boca Raton, FL.

Holman, J. P. (1989). *Heat Transfer*, pp. 231, 292, 295. McGraw-Hill, Singapore.

Iqbal, A., Decuypere, I. E., Abd El Azim, A. & Kühn, E. R. (1990). Pre- and post-hatch high temperature exposure affects the thyroid hormones and corticosterone response to acute heat stress in growing chicken (*Gallus domesticus*). *J. Therm. Biol.*, Vol. 15, No. 2, pp. 149–153.

Klir, J. J. & Heath, J. E. (1992). An infrared thermographic study of surface temperature in relation to thermal stress in three species of foxes: the red fox (*Vulpes vulpes*), arctic fox (*Alopex lagopus*), and kit fox (*Vulpes macrotis*). *Physiol. Zool.*, Vol. 65, pp. 1011–1021.

Klir, J. J., Heath, J. E. & Benanni, N. (1990). An infrared thermographic study of surface temperature in relation to thermal stress in the Mongolian gerbil, *Meriones unguiculatus*. *Comp. Biochem. Physiol.*, Vol. 96A, pp. 141–146.

Kontos, M., Wilson, R. & Fentiman, I. (2011). Digital infrared thermal imaging (DITI) of breast lesions: sensitivity and specificity of detection of primary breast cancer. *Clin. Radiol.*, Vol. 66, pp. 536–539.

Marder, J. & Arad, Z. (1989). Panting and acid-base regulation in heat stressed birds. *Comp. Biochem. Physiol.*, Vol. 94, pp. 395–400.

McCafferty, D. J., Gilbert, C., Paterson, W., Pomeroy, P. P., Thompson, D., Currie, J. I. & Ancel, A. (2011). Estimating metabolic heat loss by combining infrared thermography with biophysical modeling. *Comp. Biochem. Physiol. A.*, Vol. 158, pp. 337–345.

Minne, B. & Decuypere, E. (1984). Effects of late prenatal temperatures on some thermoregulatory aspects in young chickens. *Arch. Exp. Vet.*, Vol. 38, pp. 374–383.

Mohler, F. S. & Heath, J. E. (1988). Comparison of IR thermography and thermocouple measurement of heat loss from rabbit pinna. *Am. J. Physiol.*, Vol. 254, pp. 389–395.

Monteith, J. L. & Unsworth, M. H. (1990). *Principals of Environmental Physics*, 291 pp., Edward Arnold, London.

Morrison, S. F., Nakamura, K. & Madden, C. J. (2008). Central control of thermogenesis in mammals. *Experimental Physiology*, Vol. 93, pp. 773–797.

Nguyen, A. V., Cohen, N. J., Lipman, H., Brown, C. M., Molinari, N. A., Jackson, W. L., Kirking, H., Szymanowski, P., Wilson, T. W., Salhi, B. A., Roberts, R. R., Stryker, D. W. & Fishbein, D. B. (2010). Comparison of 3 infrared thermal detection systems and self-report for mass fever screening. *Emerg. Infect. Dis.*, Vol. 16, No. 11, pp. 1710–1717.

Nichelmann, M. (2004). Activation of thermoregulatory control elements in precocial birds during the prenatal period. *J. Therm. Biol.*, Vol. 29, pp. 621–627.

Ophir, E., Arieli, Y., Marder, J. & Horowitz, M. (2002). Cutaneous blood flow in the pigeon *Columba livia*: its possible relevance to cutaneous water evaporation. *J. Exp. Biol.*, Vol. 205, pp. 2627–2636.

Ozisik, M. N. (1985). Heat Transfer – A Basic Approach. McGraw-Hill, Singapore.

Phillips, P. K. & Heath, J. E. (1992). Heat loss by the pinna of the African elephant (*Loxodonta africana*). *Comp. Biochem. Physiol.*, Vol. 101A, pp. 693–699.

Phillips, P. K. & Sanborn, A. F. (1994). An infrared, thermographic study of surface temperature in three ratites: ostrich, emu and double-wattled cassowary. *J. Therm. Biol.*, Vol. 19, pp. 423–430.

Piestun, Y., Shinder, D., Ruzal, M., Halevy, O., Brake, J. & Yahav, S. (2008). Thermal manipulations during broiler embryogenesis: effect on the acquisition of thermotolerance. *Poultry Science*, Vol. 87, pp. 1516–1525.

Piestun, Y., Halevy, O. & Yahav, S. (2009). Thermal manipulations of broiler embryos – the effect on thermoregulation and development during embryogenesis. *Poultry Science*, Vol. 88, pp. 2677–2688.

Richards, M. P. & Proszkowiec-Weglarz, M. (2007). Mechanisms regulating feed intake, energy expenditure, and body weight in poultry. *Poultry Science*, Vol. 86, pp. 1478–1490.

Richards, S. A. (1968). Vagal control of thermal panting in mammals and birds. *J. Physiol.*, Vol. 199, pp. 89–101.

Richards, S. A. (1970). The biology and comparative physiology of thermal panting. *Biol. Rev. Camb. Philos. Soc.*, Vol. 45, pp. 223–264.

Richards, S. A. (1976). Evaporative water loss in domestic fowls and its partition in relation to ambient temperature. *J. Agric. Sci.*, Vol. 87, pp. 527–532.

Seymour, R. S. (1972). Convective heat transfer in the respiratory systems of panting animals. J. Theor. Biol., Vol. 35, pp. 119–127.

Shinder, D., Luger, D., Rusal, M., Rzepakovsky, V., Bresler V. & Yahav S. (2002). Early age cold conditioning in broiler chickens (Gallus domesticus): thermoregulatory and growth responses. J. Therm. Biol., Vol. 27, pp. 517-523.

Shinder, D., Rusal, M., Tanny, Y., Druyan, D. & Yahav, S. (2007). Thermoregulatory response of chicks (*Gallus domesticus*) to low ambient temperatures at an early age. *Poultry Science*, Vol. 86, pp. 2000–2009.

Shinder, D., Rusal, M., Giloh, M. & Yahav, S. (2009). The effect of repetitive acute cold exposures at the latest phase of embryogenesis of broilers on cold resistance during life span. *Poultry Science*, Vol. 88, pp. 636–646.

Silva, J. E. (2006). Thermogenic mechanisms and their hormonal regulation. *Physiol. Rev.*, Vol. 86, pp. 435–464.

Stewart, M., Webster, J. R., Schaefer, A. L., Cook, N. J. & Scott, S. L. (2005). Infrared thermography as a non-invasive tool to study animal welfare. *Anim. Welf.*, Vol. 14, pp. 319–325.

Tazawa H, & Nakagawa S. (1985). Response of egg temperature, heart rate and blood pressure in the chick embryo to hypothermal stress. *J. Comp. Physiol. B*, Vol. 155, pp. 195–200.

Tazawa H., Moriya, K., Tamura, A., Komoro, T. & Akiyama, R. (2001). Ontogenetic study of thermoregulation in birds. *J. Therm. Biol.*, Vol. 26, pp. 281–286.

Teunissen, L. P. J. & Daanen, H. A. M. (2011). Infrared thermal imaging of the inner canthus of the eye as an estimator of body core temperature. *J. Med. Eng. Technol.*, Vol. 35, No. 3-4, pp. 134–138.

Tzschentke, B. (2007). Attainment of thermoregulation as affected by environmental factors. *Poultry Science*, Vol. 86, pp. 1025–1036.

Tzschentke, B. & Halle, I. (2009). Influence of temperature stimulation during the last 4 days of incubation on secondary sex ratio and later performance in male and female broiler chicks. *British Poultry Science,* Vol. 50, pp. 634–640.

Tzschentke, B., & Nichelmann, M. (1997). Influence of prenatal and postnatal acclimation on nervous and peripheral thermoregulation. *Ann. N. Y. Acad. Sci.*, Vol. 813, pp. 87–94.

Tzschentke, B. & Plagemann, A. (2006). Imprinting and critical periods in early development. *World Poult. Sci. J.*, Vol. 62, pp. 626–638.

van Brecht, A., Hens, H., Lemaire, J. L., Aerts, J. M., Degraeve, P. & Berckmans, D. (2005). Quantification of the heat exchange of chicken eggs. *Poultry Science,* Vol. 84, pp. 353–361.

Webster, M. D. & King, J. R. (1987). Temperature and humidity dynamics of cutaneous and respiratory evaporation in pigeons, *Columba livia*. *J. Comp. Physiol.*, Vol. 157, pp. 253–260.

Wolfenson, D., Bachrach, D., Maman, M., Graber, Y. & Rozenboim, I. (2001). Evaporative cooling of ventral regions of the skin in heat-stressed laying hens. *Poultry Science,* Vol. 80, pp. 958–964.

Yahav, S. (2009). Alleviating heat stress in domestic fowl - different strategies. *World Poult. Sci. J.*, Vol. 65, pp. 719–732.

Yahav, S., & Hurwitz, S. (1996). Induction of thermotolerance in male broiler chickens by temperature conditioning at an early age. *Poultry Science,* Vol. 75, pp. 402–406.

Yahav, S., Goldfeld, S., Plavnik, I. & Hurwitz, S. (1995). Physiological responses of chickens and turkeys to relative humidity during exposure to high ambient temperature. *J. Therm. Biol.*, Vol. 20, pp. 245–253.

Yahav, S., Luger, D., Cahaner, A., Dotan, M., Rusal, M. & Hurwitz. S. (1998). Thermoregulation in naked neck chickens subjected to different ambient temperatures. *British Poultry Science,* Vol. 39, pp. 133–138.

Yahav, S., Straschnow, A., Luger, D., Shinder, D., Tanny, J. & Cohen, S. (2004). Ventilation, sensible heat loss, broiler energy, and water balance under harsh environmental conditions. *Poultry Science,* Vol. 83, pp. 253–258.

Yahav, S., Shinder, D., Tanny, J. & Cohen, S. (2005). Sensible heat loss: the broiler's paradox. *World Poultry Science J.,* Vol. 61, pp. 419–434.

Yahav, S., Shinder, D., Ruzal, M., Gilo, M. & Piestun, Y. (2009). Controlling body temperature – the opportunities for highly productive domestic fowl, In: *Body Temperature Control*. Cisneros, A. B. &. Goins, B. L (Eds.), pp. 65-98, Nova Science Publishers, New York.

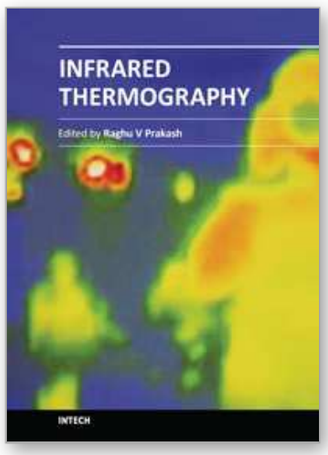

Infrared Thermography

Edited by Dr. Raghu V Prakash

ISBN 978-953-51-0242-7
Hard cover, 236 pages
Publisher InTech
Published online 14, March, 2012
Published in print edition March, 2012

Infrared Thermography (IRT) is commonly as a NDE tool to identify damages and provide remedial action. The fields of application are vast, such as, materials science, life sciences and applied engineering. This book offers a collection of ten chapters with three major sections - relating to application of infrared thermography to study problems in materials science, agriculture, veterinary and sports fields as well as in engineering applications. Both mathematical modeling and experimental aspects of IRT are evenly discussed in this book. It is our sincere hope that the book meets the requirements of researchers in the domain and inspires more researchers to study IRT.

How to reference

In order to correctly reference this scholarly work, feel free to copy and paste the following:

S. Yahav and M. Giloh (2012). Infrared Thermography - Applications in Poultry Biological Research, Infrared Thermography, Dr. Raghu V Prakash (Ed.), ISBN: 978-953-51-0242-7, InTech, Available from: http://www.intechopen.com/books/infrared-thermography/infrared-thermography-applications-in-agriculture-and-biological-research

INTECH
open science | open minds

InTech Europe
University Campus STeP Ri
Slavka Krautzeka 83/A
51000 Rijeka, Croatia
Phone: +385 (51) 770 447
Fax: +385 (51) 686 166
www.intechopen.com

InTech China
Unit 405, Office Block, Hotel Equatorial Shanghai
No.65, Yan An Road (West), Shanghai, 200040, China
中国上海市延安西路65号上海国际贵都大饭店办公楼405单元
Phone: +86-21-62489820
Fax: +86-21-62489821

IntechOpen